Proceedings of PRADS2016
4th – 8th September, 2016
Copenhagen, Denmark

# Methods for preliminary analysis of floating bridge structures

Thomas H. Viuff [1)], Bernt J. Leira [1)], Xu Xiang [2)] and Ole Øiseth [1)]

[1)] Norwegian University of Science and Technology, Norway
[2)] Norwegian Public Roads Administration, Norway

## Abstract

*A theoretical overview of the stochastic dynamic analysis of a floating bridge structure is presented. Emphasis is on the wave-induced response for waves on the sea surface idealized as a zero mean stationary Gaussian process. The first-order wave load processes are derived using linear potential theory and the structural idealization is based on the Finite Element Method. A discussion of the frequency response method and the impulse response method as solution techniques to solve the equation of motion is presented. A case study of a simplified floating bridge structure is presented with results from the frequency response method. The numerical example emphasizes the influence from low- and high frequency waves and frequency dependence in hydrodynamic added mass and damping coefficients.*

## Keywords

Floating; pontoon; bridge; linear; dynamic; stress; response.

## Introduction

Floating bridges have been around for many thousands of years and throughout the years, they have been used as temporary supply lines or for military purposes. However, it is only during the last three decades or so that floating bridges are being developed to the degree of sophistication, so they can be applied as a critical part of modern infrastructure. Still, compared with land-based bridges, including cable-stayed bridges, limited information (Skorpa, 2010) is currently available on floating bridges and even less on submerged floating tunnels for transportation. This information is especially true regarding construction records, environmental conditions, durability, operations and performance of the structure.

The limited amount of floating bridges currently in the world is a statement to this fact. Depending on the landscape in the proximity of the floating bridge and on the sea state conditions different types of floating bridges are used. Only three long span floating bridges are currently located in difficult sea state conditions and allows for cars to pass. These are:

i. Hood Canal Bridge (1961) in USA a 2,398 meter long pontoon bridge with a 1,988 meter long anchored floating portion, it is the longest floating bridge in the world located in a saltwater tidal basin, and the third longest floating bridge overall.
ii. Bergsøysund Bridge (1992) in Norway a 931 meter long pontoon bridge with the longest span of 106 meters.
iii. Nordhordland Bridge (1994) in Norway is a combination of a cable-stayed and pontoon bridge. It is the longest free floating bridge without anchorage.

As the rough overview indicates, the theoretical and practical development of floating bridges has been carried out mainly in USA and in Norway with significant contributions from the industry. In Norway it is mainly the Norwegian University of Science and Technology (NTNU), SINTEF the research organisation and the Norwegian Public Roads Administration (NPRA).

Pioneering studies on floating bridges was carried out by Hartz in the 1970's. Around the same time Holand, Sigbjörnsson and Langen carried out similar studies on stochastic dynamics of floating bridges (Holand, 1972). Later on in 1980 Sigbjörnsson and Langen exemplified the theory using a model of the Salhus floating bridge (Langen and Sigbjörnsson, 1980).

In recent years NTNU/SINTEF have led the theoretical evolution within structural mechanics, fluid structure interaction and stochastic modelling of environmental loads applied to the offshore industry in Norway. Many of the same theories can be directly applied in stochastic dynamic analysis of floating bridges.

In the present text a dynamic analysis in frequency domain will be given and theory on stochastic dynamic modelling of a floating bridge is described, including challenges regarding frequency-dependent hydrodynamic added mass and damping. Preliminary results will be given from a frequency domain analysis of the local stresses on the pontoon.

## System Modelling

The linear stochastic dynamic response of a floating bridge structure can be described using the equation of motion to capture the dynamics of the structure, potential theory to find the hydrodynamic added mass and

damping and the wave excitation force from the fluid-structure interaction and stochastic theory to implement the randomness of the wave excitation force.

***Equation of Motion***

The equation of motion describing the linear dynamic behaviour of the floating bridge is described in time domain as shown in Eq. 1.

$$[M_s]\{\ddot{u}(t)\}+[C_s]\{\dot{u}(t)\}+[K_s]\{u(t)\}=\{q_h(t)\} \tag{1}$$

Here, $[M_s]$, $[C_s]$ and $[K_s]$ are the frequency independent structural mass-, damping- and stiffness matrices. The vector notation $\{u\}$ is the structural response and the dots above represents derivatives of time $t$. The vector $\{q_h(t)\}$ represents the hydrostatic and hydrodynamic load vector.

For a single harmonic small amplitude wave, $\{q_h(t)\}$ can be described as a harmonic wave proportional to floater motion as shown in Eq. 2. As an extra step in the equation, the derivatives of the structural response are derived and collected within the parenthesis.

$$\begin{aligned}\{q_h(t)\} = &-\left(-\omega^2[M_h(\omega)]+i\omega[C_h(\omega)]+[K_h]\right)\\ &\cdot\{Z_u(\omega)\}e^{i\omega t}+\{Z_q(\omega)\}e^{i\omega t}\end{aligned} \tag{2}$$

Here, $[M_h(\omega)]$ and $[C_h(\omega)]$ are the frequency dependent hydrodynamic added mass and damping and $\omega$ is the angular frequency. $[K_h]$ is the restoring stiffness assumed frequency independent for small amplitude motion. $\{Z_u(\omega)\}$ and $\{Z_q(\omega)\}$ are the complex structural response amplitude and the complex wave excitation force amplitude, respectively, and $i$ is the imaginary unit. Substituting the expression for the hydrodynamic action given in Eq. 2 into the equation of motion in Eq. 1 and rearranging the terms gives the frequency domain representation of the equation of motion.

$$\{Z_q(\omega)\}=\left[-\omega^2[M(\omega)]+i\omega[C(\omega)]+[K]\right]\{Z_u(\omega)\} \tag{3}$$

The inertia, damping and restoring matrices include the structural terms as well as the hydrodynamic added mass and damping. The combined system matrices are hence given as:

$$[M(\omega)]=[M_s]+[M_h(\omega)] \tag{4}$$

$$[C(\omega)]=[C_s]+[C_h(\omega)] \tag{5}$$

$$[K]=[K_s]+[K_h] \tag{6}$$

The response induced by a single harmonic wave is then obtained by rearranging the terms in Eq. 3 and introducing the frequency transfer function $[H(\omega)]$.

$$\{Z_u(\omega)\}=[H(\omega)]\{Z_q(\omega)\} \tag{7}$$

$$[H(\omega)]=\left[-\omega^2[M(\omega)]+i\omega[C(\omega)]+[K]\right]^{-1} \tag{8}$$

By use of the principle of superposition, it is possible within the framework of linear theory to incorporate a generalized description of the excitation represented as the sum of a finite number of harmonic waves. In case of a random sea state the excitation in frequency domain can be obtain by Fourier transform of the excitation time series.

Assuming frequency independent restoring and causality the wave excitation force can be described in the time domain as shown in Eq. 9 by use of the convolution integral.

$$\begin{aligned}\{q_h(t)\} = \{q(t)\} &- \int_{-\infty}^{+\infty}[m_h(t-\tau)]\{\ddot{u}(t)\}d\tau\\ &-\int_{-\infty}^{+\infty}[c_h(t-\tau)]\{\dot{u}(t)\}d\tau-[K_h]\{u(t)\}\end{aligned} \tag{9}$$

Here, $\tau$ is time lag and $[m_h]$ and $[c_h]$ are the time domain representations of the hydrodynamic added mass and damping found from Fourier transform.

$$[m_h(\mathrm{t})]=\frac{1}{2\pi}\int_{-\infty}^{+\infty}[M_h(\omega)]e^{i\omega t}d\omega \tag{10}$$

$$[c_h(t)]=\frac{1}{2\pi}\int_{-\infty}^{+\infty}[C_h(\omega)]e^{i\omega t}d\omega \tag{11}$$

Using the impulse response function, $h(\cdot)$, the response can be obtained in time domain as a finite sum of system responses from hydrodynamic action impulses at different time steps.

$$\{u(t)\}=\int_{-\infty}^{+\infty}[h(t-\tau)]\{q_h(\tau)\}d\tau \tag{12}$$

The impulse response function is found from Fourier transform of the frequency transfer function in Eq. 8.

$$[h(t)]=\frac{1}{2\pi}\int_{-\infty}^{+\infty}[H(\omega)]e^{i\omega t}d\omega \tag{13}$$

Several methods exist to solve Eq. 9 in time domain. Such approaches are useful if non-linear behaviour is of interest.

***Description of Sea Waves***

For engineering purpose, the wind-generated waves are approximated as a locally stationary and homogeneous random field and the sea surface elevation $\eta(\{x\},t)$ becomes a function of time and the two-dimensional space vector for the horizontal surface at the mean water level.

$$\eta(\{x\},t)=\int_{-\infty}^{+\infty}e^{\mathrm{i}(\{\kappa\}\{\mathrm{x}\}-\omega\,\mathrm{t})}dZ_\eta(\{\kappa\},\omega) \tag{14}$$

Here, $Z_\eta(\{\kappa\},\omega)$ is the spectral process of the sea surface elevation and $\{\kappa\}=\{\kappa_x,\kappa_y\}$ is the two-dimensional wave number vector.

The spectral process is, given the assumptions of stationarity and homogeneity, related to wave spectral density $S_{\eta_r\eta_s}(\{\kappa\},\omega)$ as described in Eq. 15.

$$E\left[dZ_{\eta_r}(\{\kappa\},\omega)dZ^{T*}_{\eta_s}(\{\kappa\},\omega)\right] = S_{\eta_r\eta_s}(\{\kappa\},\omega)d\kappa_x d\kappa_y d\omega \tag{15}$$

Here, the subscripts $r$ and $s$ refer to points in time and space. The superscripts $T$ and * refer to the mathematical operations transpose and complex conjugate, respectively. The operation $E[\cdot]$ is the expected value.

The wave spectral density is divided into a cross-spectral term with $r \neq s$ and auto-spectral terms with $r = s$. The auto-spectral density is denoted $S_\eta(\omega,\theta)$.

The wave number vector can be described as a function of the wave direction $\theta$ and the modulus $\kappa$.

$$\{\kappa\} = \begin{Bmatrix}\cos\theta \\ \sin\theta\end{Bmatrix}\kappa \tag{16}$$

Furthermore, within the 1st order Stokes theory $\kappa$ and $\omega$ are related through the dispersion relationship given in Eq. 17.

$$\omega^2 = g\kappa\tanh(\kappa h) \tag{17}$$

Here, $g$ is the gravitational acceleration and $h$ is the water depth. In the special case of deep water waves the dispersion relationship can be approximated as $\kappa \approx \omega^2 g^{-1}$. As a result of this approximation the spectral density can be described as a function of wave direction and frequency.

The auto-spectral density is generally a function of the frequency-dependent directional distribution $D(\omega,\theta)$ and the one-dimensional wave spectral density $S_\eta(\omega)$. For simplicity, the directional distribution is normally assumed to be frequency-independent as given in Eq. 18.

$$\mathrm{S}_\eta(\omega,\theta) = S_\eta(\omega)D(\theta) \tag{18}$$

Due to the coherency between point $r$ and $s$ the expression for the cross-spectral density given in Eq. 19 is a bit more complicated and is formulated by assuming deep water waves.

$$S_{\eta_r\eta_s}(\omega,\theta) = S_{\eta_r\eta_s}(\omega)Coh_{\eta_r\eta_s}(\omega)$$
$$Coh_{\eta_r\eta_s}(\omega) = \int_{-\pi}^{+\pi} D(\theta)e^{-i\frac{|\omega|\kappa(\omega)}{g}(\Delta x\cos\theta+\Delta y\sin\theta)}d\theta \tag{19}$$

Here, $\Delta x$ and $\Delta y$ are the horizontal distances between point $r$ and $s$.

The directional distribution is commonly characterised by a bell shaped function centered around the mean wave direction. The simplest and one of the most commonly applied functional forms is the so-called cos-2s distribution, given in Eq. 20 for a specific mean wave direction.

$$D(\theta) = \frac{2^{2s-1}}{\pi}\frac{\Gamma^2(s+1)}{\Gamma(2s+1)}\cos^{2s}\left(\frac{\theta-\theta_m}{2}\right)$$
$$\pi \le (\theta-\theta_m) \le \pi \tag{20}$$

Here, $s$ is the spreading parameter, $\Gamma(\cdot)$ is the Gamma function and $\theta_m$ is the mean wave direction.

***Fluid Structure Interaction***

The current analysis of floating bridges is based on the assumption of water being incompressible, non-viscous and irrotational. Then, within the framework of potential theory, the flow field is governed by Laplace's equation, given in Eq. 21 for Cartesian coordinates.

$$\nabla^2\Phi = \frac{\partial^2\Phi}{\partial x^2}+\frac{\partial^2\Phi}{\partial y^2}+\frac{\partial^2\Phi}{\partial z^2} = 0 \tag{21}$$

Here, $\Phi$ is the velocity potential and $x$, $y$ and $z$ are Cartesian coordinates. Hence, the basic problem at hand is to find the solution of the Laplace's equation in terms of the velocity potential.

Assuming no current and by virtue of the principle of superposition the velocity potential can be obtained the linear problem given in Eq. 22.

$$\Phi = \underbrace{\varphi_0 e^{-i\omega t} + \varphi_7 e^{-i\omega t}}_{\text{diffraction problem}} + \underbrace{\sum_{k=1}^{6}\phi_k\dot{u}_k}_{\text{radiation problem}} \tag{22}$$

Here, $\varphi_0$ and $\varphi_7$ represents the velocity potential from the incident- and diffracted waves, respectively. $\phi_k$ represents the velocity potential per unit velocity from radiated waves and $\dot{u}_k$ represents the time derivative of the complex motion of the body in the water and together they represent the velocity potential from radiated waves $\varphi_k = \phi_k\dot{u}_k$ when the body is oscillating in the $k$'th degree of freedom.

From 1st order Stokes theory the velocity potential for the incident wave is known. To obtain a physical legitimate solution for the other seven velocity potentials in Eq. 22 the Laplace's equation in Eq. 21 must be satisfied together with the free-surface boundary condition at the mean water level, the kinematic boundary conditions at the seabed and on the wetted body surface and the radiation condition. Using the indirect boundary integral formulation and applying Green's second identity it is possible to obtain solutions for each of the seven velocity potentials and the pressure $p$ can then be obtained through Bernoulli's equation.

$$p = -\rho gz - \rho\frac{\partial\varphi}{\partial t} \tag{23}$$

Here, $\rho$ represents the water density, $z$ is the vertical position from the mean water level and $\varphi$ represents any of the seven velocity potentials. Applying specific velocity potentials in Eq. 23 and integrating the hydrodynamic pressure over the wetted body surface it is possible to obtain expressions for the wave excitation force and the hydrodynamic added mass and damping when comparing to the equation for steady-state harmonic rigid body motion is given in Eq. 24.

$$q_j e^{-i\omega t} = \sum_{k=1}^{6}\left(M_{jk}(\omega)\ddot{u}_k + C_{jk}(\omega)\dot{u}_k + K_{jk}u_k\right) \tag{24}$$

Here, the index notations of Eqs. 4~6 is applied. The diffraction problem describes the scenario of a fixed

body in incident waves. By only including $\varphi_0$ and $\varphi_7$ in Eq. 23 it is possible to obtain the hydrodynamic action by integrating the hydrodynamic pressure over the wetted body surface $S_0$.

$$q_j = -i\omega\rho \int_{S_0} (\varphi_0 + \varphi_7) n_k dS \tag{25}$$

Here, $n_k$ represents the component of the surface normal vector in the direction of the $k$'th degree of freedom. Comparing the expression with Eq. 24 the force is identified as the wave excitation force.

The radiation problem describes the scenario of a body oscillating in calm sea. Using the same approach the hydrodynamic action from a body oscillating in calm water can be found.

$$\begin{aligned} q_j &= -i\omega\rho\dot{u}_j \int_{S_0} \phi_j n_k dS \\ &= \underbrace{\rho \,\mathrm{Re}\left( \int_{S_0} \phi_j n_k dS \right)}_{M_{h,jk}(\omega)} \ddot{u}_j + \underbrace{\rho\omega \,\mathrm{Im}\left( \int_{S_0} \phi_j n_k dS \right)}_{C_{h,jk}(\omega)} \dot{u}_j \end{aligned} \tag{26}$$

Comparing the expression with Eq. 24 the hydrodynamic added mass and damping can be identified.

## Hydrodynamic Interaction between Pontoons

A floating bridge may have multiple pontoons such as the Bergsøysund Bridge. The total length of the bridge is around 931 meters and the longest span between each pontoon is 106 meters. An issue for such a multi-body floating bridge system is the hydrodynamic interaction between the pontoons. A straightforward way of accounting for this effect is to solve for the velocity potential with all the pontoons hydrodynamically coupled. This can be done by extending the radiation part of Eq. 22 to include $n$ bodies, where $n$ is the number of pontoons. The corresponding radiation potential will include $6n$ components. Generally speaking, the interaction effects may result to extra peaks on the added mass, damping coefficients, and wave loads, as shown by Xiang and Faltinsen (2011) by studying a side-by-side two floaters system. The peaks can be related to the piston and sloshing modes of the restricted water body between the floaters, for which more comprehensive analysis can be found in Faltinsen and Timokha (2009).

In practice, the relative dimensions of the pontoons compared to the distance between them will govern whether the interaction effects should be accounted for or not. A simple estimation is referred to in Xiang (2012) where two pontoons are considered to be hydrodynamically interacting when the following equation is satisfied:

$$D_{AB} \le D_{INT} = \sqrt{\left(1.5\frac{L_A + L_B}{2}\right)^2 + \left(6\frac{B_A + B_B}{2}\right)^2} \tag{27}$$

Here $L_A$, $L_B$, $B_A$ and $B_B$ are the length and width of pontoon $A$ and $B$, respectively. The equation is based on the experience of the author's calculation on coupled motions of two interacting ships, Xiang (2012). The hydrodynamic interaction effects will generally be insignificant out of this range. Using the Bergsøysund Bridge as an example, 34 m and 20 m the length and width of both pontoons, we get $D_{INT} = 130.4$ m. This means that we have to consider the pontoons hydrodynamically dependent on each other. In addition, the pontoons are interacting with each other mechanically through the bridge structure.

## Solution Strategy

It is commonly assumed within the field of civil engineering structural dynamics, that structural damping is very small and hence can be neglected when calculating the natural frequencies and natural modes of a classically damped system. In the case of fluid structure interaction there is significant contributions to the damping from hydrodynamic damping $[C_h(\omega)]$ and so the system instead is categorised as a non-classically damped system. Procedures exists to calculate this higher order eigenvalue problem by use of the state-space approach. The solution consists of complex eigenvalues and complex eigenvectors.

In the context of this article, the dynamic response is calculated using the direct frequency response method with the structure subjected to a set of unit amplitude wave with periods ranging from 1 second to 15 seconds.

### *Direct Frequency Response Method*

The frequency domain representation applies the complex frequency transfer function $[H(\omega)]$ given in Eq. 8 to obtain solutions in the frequency domain. The response amplitude $\{Z_u(\omega)\}$ is a complex quantity describing the amplitude and the phase angle of the dynamic response. By splitting the load into a real part $\{Z_{q,\mathrm{Re}}(\omega)\}$ and an imaginary part $\{Z_{q,\mathrm{Im}}(\omega)\}$ the solution can be as shown in Eq. 28.

$$\{Z_u(\omega)\} = [H(\omega)]\{Z_{q,\mathrm{Re}}(\omega)\} + i[H(\omega)]\{Z_{q,\mathrm{Im}}(\omega)\} \tag{28}$$

## Case Study

### *Description of Floating Bridge Model*

The model is a simplified floating pontoon bridge with pontoon dimensions equal to the pontoons used in the mid sections of the Bergsøysund Bridge. The model consists of a truss system made up of four beam types and two pontoons, see Fig. 1 where the $x$-, $y$- and $z$-axis corresponds to surge, sway and heave, respectfully.

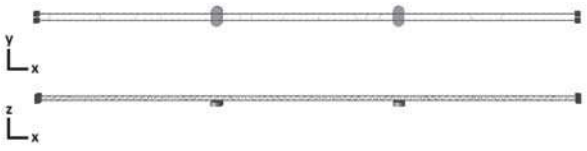


**Figure 1. Bridge layout**

The total length of the model is 896 meters and the pontoons are located 297 meters from each end. A more detailed look at the truss system is given in Fig. 2.

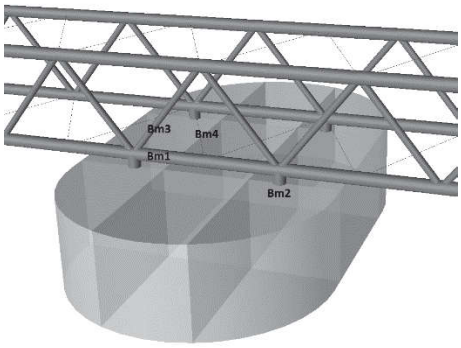


**Figure 2. Truss system**

The four beams are modelled as hollow circular cross-sections with outer diameter and thickness given in Table 1.

**Table 1: Beam element properties**

| | Outer diameter [m] | Thickness [m] |
|---|---|---|
| Beam 1 | 9.50E-01 | 5.00E-02 |
| Beam 2 | 9.50E-01 | 4.50E-02 |
| Beam 3 | 5.00E-01 | 1.50E-02 |
| Beam 4 | 2.00E-02 | 2.00E-03 |

The mass properties of the pontoon is listed in Table 2. Here, $r_{jj}$ represents the radius of gyration around the $j$'th axis.

Beam 4 is given relatively small dimensions in order to make the bridge system more flexible on the horizontal direction.

The pontoon shown in Fig. 2 is 6.98 meter high and is made of lightweight concrete with a modulus of elasticity of 50 MPa.

**Table 2. Pontoon mass properties**

| $M$ [kg] | $r_{xx}$ [m] | $r_{yy}$ [m] | $r_{zz}$ [m] |
|---|---|---|---|
| 1.37E+06 | 1.01E+01 | 6.80E+00 | 1.15E+01 |

Supports are located at each end of the floating bridge model and modelled as fixed in all degrees of freedom.

***Numerical Analysis***

Due to the hydrodynamic added mass and damping, it is crucial to know the correct pontoon draft before commencing the dynamic analysis. Therefore, a static analysis is first carried out.

From equilibrium between the pontoon mass and buoyancy from the displaced water, the initial draft of the pontoon is found. The static analysis is then carried out by replacing the pontoons with a vertical spring stiffness from the waterplane area and the water density. Applying gravitational loads to the static model the vertical displacement is computed. The final draft of the pontoon is 4.56 meters found by combining the result from the static analysis with the initial draft.

The hydrodynamic restoring, added mass and damping is calculated using a boundary element method software. A panel model of the pontoon surface as the one in Fig. 3 is created and given as input to the software. The panel model used consists of 2384 panel elements and is subjected to 60 unit amplitude waves with periods $T = \{1 : 0.25 : 15\}$ seconds each with a wave direction of 90 degrees from the global $x$-axis corresponding to sway. The water depth is set equal to 1000 meters.

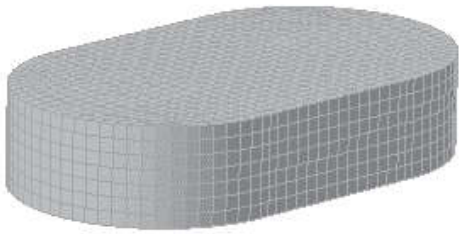

**Figure 3. Panel- and structural model of pontoon**

The mesh size of the panel model is roughly 1.00 meter, which according to Faltinsen (1990), requires a minimum wavelength of 8.00 meter or in this case an equivalent wave period of approximately 2.26 seconds.

From the analysis, information of the hydrodynamic added mass and damping as a function of frequency is illustrated in Fig. 4 as normalised values. Normalization factors are $f_m = 5.55\text{E+}06$ and $f_c = 1.74\text{E+}06$ for added mass and damping, respectively.

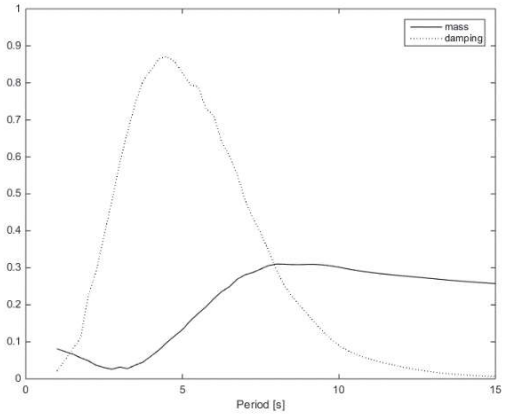


**Figure 4. Normalized hydrodynamic added mass and damping in y-direction (sway) for one pontoon**

Choosing a damping ratio of $\zeta = 0.05$ the Rayleigh damping is calibrated using the first two horizontal undamped natural periods $T_{n1} = 41.01\text{s}$ and $T_{n2} = 21.95\text{s}$ found from solving the classical eigenvalue problem.

From the sway response of the midpoint of the floating bridge, it can be checked whether appropriate structural damping is applied. It is important to have a sufficiently low mass proportional damping in order not to damp out the wave response.

## Results

From the dynamic analysis carried out in the frequency domain it is possible to obtain some preliminary results of the stress distribution in the pontoon. The stress response from a set of 60 unit amplitude mono-chromatic beam sea waves have been analysed and special characteristics of the special and frequency distribution of von Mises stress has been observed.

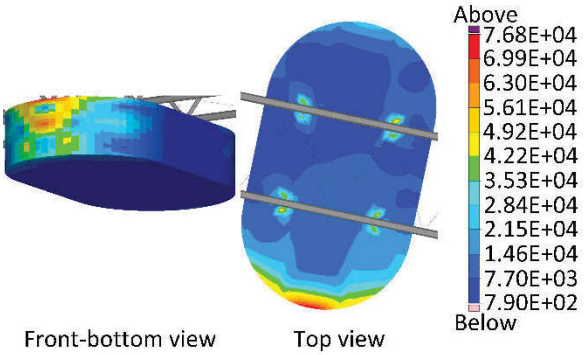


**Figure 5. Von Mises stress on pontoon for mono-chromatic wave excitation force with $T = 1.75\text{s}$. Units in Pa**

At high frequency waves (period in the range of 1 second to 3 seconds) the largest stresses in the pontoon are located in the front part of the pontoon and on the corners connecting the front vertical concrete plates to the top- and bottom concrete plates, see Fig. 5. Maximum values are in the range of 0.07 MPa.

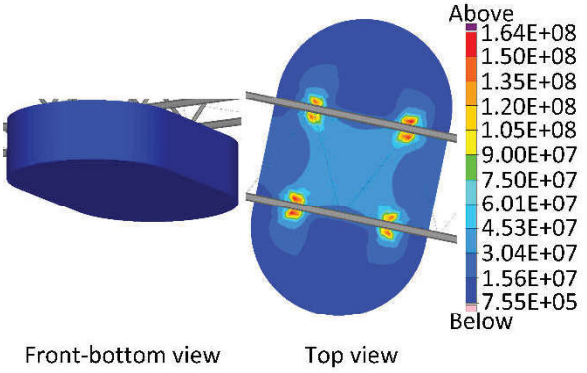


**Figure 6. Von Mises stress on pontoon for mono-chromatic wave excitation force with $T = 8.50\text{s}$. Units is Pa**

Instead, at lower frequencies the largest von Mises stress is located exclusively around the connection point between the pontoon and the vertical beam as illustrated in Fig. 6. The stresses are in this case as high as 164 MPa. It is believed that the high stress is a result of the high wave loads on the pontoon under long waves.

The minimum stresses at the low frequency wave excitation is roughly the same order as the stresses from the high frequency wave excitation force.

## Conclusion and Further Work

The paper has presented general theory on solutions of the equation of motion in both time- and frequency domain and has explained how to incorporate the randomness of the sea state into the design using stochastic theory. Also a brief discussion of how potential theory and boundary element methods can be used when dealing with a non-classically damped system such as a floating bridge structure.

A case study of a simplified floating bridge structure has been presented and preliminary results of the stress distribution on the pontoon is shown.

From the preliminary analysis in frequency domain it can be concluded from the results given in Figs. 5~6 that the joint between the pontoon and the beam bridge structure is crucial in the design of the pontoon and, if not thoughtfully carried out, can generate high stresses in the pontoon surface elements.

Although the simplified pontoon bridge is made to resemble a realistic floating bridge structure, many details are lost in the simplification, such as a proper connection between pontoon and bridge deck. Future work includes more pontoons and a stochastic dynamic analysis in frequency and time domain.

## Acknowledgement

The late Prof. Ragnar Sigbjörnsson has contributed to section *Equation of Motion* and *Description of Sea Waves* with an initial draft.

## References

Faltinsen, OM (1990). “Sea Loads on Ships and Offshore Structures”, Cambridge University Press.

Faltinsen, OM and Timokha, AN (2009). “Sloshing”, Cambridge University Press.

Holand, I and Langen, I (1972). “Salhus floating bridge: theory and hydrodynamic coefficients”, SINTEF Report. Trondheim, SINTEF.

Langen, I and Sigbjörnsson, R (1980). “On stochastic dynamics of floating bridges”, Eng. Struct..

Skorpa, L (2010). “Developing new methods to cross wide and deep Norwegian fjords”, Procedia Engineeering, Vol 4, Issue 1877, pp 81-89.

Xiang, X and Faltinsen, OM (2011) “Time domain simulation of two interacting ships advancing parallel in waves”, OMAE2011-49484. Proceedings of OMAE2011, the 30th International Conference on Ocean, Offshore and Arctic Engineering, Rotterdam, the Netherland.

Xiang, X (2012). “Maneuvering of two interacting ships in waves”. Ph.D. Thesis. Center for Ships and Ocean Structures, Norwegian University of Science and Technology.